HHS Public Access

Author manuscript

Birth Defects Res A Clin Mol Teratol. Author manuscript; available in PMC 2015 May 11.

Published in final edited form as:

Birth Defects Res A Clin Mol Teratol. 2014 August ; 100(8): 598–607. doi:10.1002/bdra.23264.

Midline craniofacial malformations with a lipomatous cephalocele are associated with insufficient closure of the neural tube in the *tuft* mouse

Keith S. K. Fong, **Dana A. T. Adachi**, **Shaun B. Chang**, and **Scott Lozanoff**

Department of Anatomy, Biochemistry, and Physiology, University of Hawaii, John A. Burns School of Medicine

Abstract

Genetic variations affecting neural tube closure along the head result in malformations to the face and brain, posing a significant impact on health care costs and the quality of life. We have established a mouse line from a mutation that arose spontaneously in our wildtype colony that we called *tuft*. *Tuft* mice have heritable midline craniofacial defects featuring an anterior lipomatous cephalocele. Whole mount skeletal stains indicated that affected newborns had a broader interfrontal suture where the cephalocele emerged between the frontal bones. Mice with a cephalocele positioned near the rostrum also presented craniofacial malformations such as ocular hypertelorism and midfacial cleft of the nose. Gross and histological examination revealed that the lipomatous cephalocele originated as a fluid filled cyst no earlier than E14.5 while embryos with a midfacial cleft was evident during craniofacial development at E11.5. Histological sections of embryos with a midfacial cleft revealed the cephalic neuroectoderm remained proximal or fused to the frontonasal ectoderm about the closure site of the anterior neuropore, indicating a defect to neural tube closure. We found the neural folds along the rostrum of E9-10.5 embryos curled inward and failed to close as well as embryos with exencephaly and anencephaly at later stages. Whole mount *in situ* hybridization of anterior markers Fgf8 and Shh indicated closure of the rostral site was compromised in severe cases. We present a model demonstrating how anterior cranial cephaloceles are generated following a defect to neural tube closure and relevance to subsequent craniofacial morphogenesis in the *tuft* mouse.

Keywords

anterior cranial cephalocele; midfacial cleft; neural tube defect; encephalocele; exencephaly; anencephaly

Introduction

A cephalocele is a rare birth defect that is characterized by a sac-like mass protruding through a defective opening in the skull. The sac varies in size that typically consists of herniated meninges and brain tissue (meningoencephalocele or encephalocele) or fragments

Correspondence: Keith S. K. Fong, Department of Anatomy, Biochemistry and Physiology, University of Hawai'i, John A. Burns School of Medicine, 651 Ilalo Street; BSB 110, Honolulu, HI 96813, ksfong@hawaii.edu, 808-692-1421.

of disorganized neural tissue. Alternatively, the sac may contain only the meninges (cranial meningocele) or it may include part of the ventricle filled with CSF (encephalocystocele) covered by skin. In the latter cases, the underlying brain is usually structurally intact. Although cephaloceles have been classified and described as a neural tube defect (NTD), since it shares similar characteristics seen resulting in anencephaly and spina bifida, its pathogenesis is not clearly understood.

Encephaloceles occur at a rate of approximately 1 in 10,000 live births in the US, or about 1 in 5,000 worldwide (CDC, NINDS, March of Dimes, Rowland et al., 2006). The true incidence, however, is probably higher since an estimated 70% do not survive (Singh and Upadhyaya 2009). Encephaloceles can be detected by ultrasound and the fetus is usually opted for abortion. Despite declining frequencies, largely due to prenatal supplementation of folic acid, NTDs remain among the most common serious defects (Thompson 2009; Harris and Juriloff 2010). Recent statistics indicate, however, that prenatal supplementation of folic acid may not have a significant impact on the rate of encephaloceles (Rowland et al., 2006). This suggests that genetic and environmental factors are significant contributors to the occurrence of this deadly disorder. Identifying the genes that are affected may lead to preventive measures.

Cranial cephaloceles can emerge anywhere along the midline suture of the skull and are classified based on their location. Anterior encephaloceles are commonly found emanating from the junction of the frontal and ethmoid bones (frontoethmoidal encephaloceles) about the bridge of the nose, whereas occipital encephaloceles emerge from the sutures in the occipital region near the hindbrain. Occipital encephaloceles are more common in Caucasian populations of Western European ancestry (North America, Europe and Australia), whereas anterior encephaloceles appear more common in Southeast Asia (Suwanwela and Suwanwela 1972; Mahapatra and Agrawal 2006; Singh and Upadhyaya 2009). Occipital encephaloceles are also prominent features of Knobloch syndrome (KS) and Meckel-Gruber syndrome (MKS). KS is characterized by progressive ocular abnormalities leading to blindness that can be caused by mutations in the COL18A1 gene (Sertie et al., 2000). MKS is considered to be the most common syndromic form of NTDs that can also present midline facial defects such as cleft lip and palate (reviewed in Logan et al., 2011). Mutations affecting the function of primary cilia have been found in MKS cases, but its significance to cephalocele formation is yet to be explained. Because of their location, anterior encephaloceles can also occur together with craniofacial malformations such as frontonasal dysplasia (Suwanwela and Suwanwela 1972; Cohen and Lemire 1982; Guion-Almeida et al., 1996; Cohen 2002; Dutta et al., 2010). Currently, there are no animal models to explain the etiology of anterior cephaloceles.

We recently described the *tuft* mouse with heritable craniofacial malformations resembling frontonasal dysplasia (FND) featuring an interhemispheric lipoma. Affected adults exhibited one or more craniofacial malformations that included ocular hypertelorism, frontonasal cleft (bifid nose), shortened and sloping nasal ridge, and a lipomatous extracranial mass emanating from the anterior part of the skull (Fong et al., 2012). Histological and imaging analysis indicated that the lipomatous mass was an extension of the meninges protruding through an opening along the sagittal suture, usually between the paired frontal bones of the

mouse. Its occurrence was associated with a frontonasal cleft when proximal to the nasal field. We examined their origins during embryonic development and here we show these malformations were also associated with insufficient closure of the anterior part of the neural tube. Thus, the *tuft* mouse provides a novel animal model to identify genes and pathways involved with forebrain closure and understand the pathogenesis of cranial cephaloceles.

Methods

Animals

All procedures were carried out in accordance with IACUC specifications and performed following protocols approved by the University of Hawai'i Laboratory of Animal Services. Mice strains were housed under standard conditions and bred as previously described (Fong et al., 2012). Timed matings were determined by noting the presence of a vaginal plug as day 0.5 for staging embryo collections and estimating date of births. Developmental stages of embryos were determined according to Theiler (Theiler 1989).

Histology

Whole mount staining of newborn skulls with Alcian blue and Alizarin Red were previously described (Fong et al., 2012). Each mouse cranium was observed with a Leitz dissection microscope and digitally documented (Olympus Imaging America Inc., Center Valley, PA).

Embryos were dissected at various developmental stages between E9.0-17.5 for histological examination by standard hematoxylin and eosin staining for gross cellular organization or immunohistochemistry for specific protein localizations. Essentially, samples were fixed in 4% paraformaldehyde for several hours at room temperature or overnight at 4°C. Samples were subsequently washed in PBS and dehydrated stepwise to 70% ethanol, 100% methanol or cryoprotected with 30% sucrose at 4°C. Samples were then embedded in paraffin or O.C.T. freezing medium (Sakura Finetek, Torrence, CA) and serially sectioned into 10 μm slices for staining using conventional methods. Sections were immunostained with anti-laminin antibody diluted 1:1000 (Sigma-Aldrich, St. Louis, MO), anti-E-cadherin (Cell Signaling Technology, Danvers, MA) diluted 1:200, anti-N-cadherin (EMD Millipore, Billerica, MA) diluted 1:400, and counterstained with 1:200 phalloidin (Biotium, Hayward, CA) for actin and 600 nM DAPI (Invitrogen Life Technologies, Grand Island, NY) for nuclei. Primary antibodies were indirectly localized using DyLight donkey anti-rabbit-488 secondary antibodies (Jackson ImmunoResearch, West Grove, PA) diluted 1:1000 and visualized with an Olympus BX41 fluorescence microscope.

Embryo litters stored in methanol were used to detect RNA with digoxigenin-labeled riboprobes by whole mount *in situ* hybridization (WMISH) based on procedures described elsewhere (Correia and Conlon 2001; Lufkin 2007) and the manufacturer's specifications (Roche Applied Science, Indianapolis, IN).

Experimental Results

1. Anterior cephaloceles were associated with defects of cranial development

The defects exhibited by adult *tuft* mice were visible at birth. Affected newborn pups either had a cranial swelling resembling a cephalocele, midfacial cleft, or both. A single bump covered with skin was seen on the surface of the head of varying size along the midline axis, usually coinciding with the interfrontal suture between the frontal bones (Figure 1A and B). It had the appearance of a cyst or hematoma as it darkened with tissue and sometimes with blood. Size of the cephalocele varied and correlated with the animal's viability, since pups with larger swellings usually had poor prognosis or died before maturing. Mice with a cephalocele positioned closer to the nose usually exhibited a midfacial cleft separating the rostrum and upper lip of varying severity (Figure 1C, D). Whereas mice with a cephalocele or smaller cyst located further from the nose toward the hindbrain did not exhibit craniofacial malformations. Cephaloceles were usually located near the rostrum in affected *tuft* mice and rarely beyond the frontal-parietal bone junction.

Nearly 40% of the affected newborn pups had a midfacial cleft separating the rostrum and upper lip (Table 1), indicating the defect could disrupt the merging or fusion of the medial nasal and maxillary prominences during embryogenesis. Cleft width varied, but was usually severe enough that pups were unable to be nursed and died within 48 hrs. Mild clefts that resulted in bifid noses were relatively uncommon and subtle to detect at birth, occurring less than 10% of all affected mice (**data not shown**). An anterior cephalocele or swelling resembling a small blister or hematoma was almost always visible in mice with a severe cleft (Compare Figures 1C and D). Stillborns with anencephaly were also observed in some cases, occurring together with a midfacial cleft more than 50% of the time (Table 1 **and data not shown**). Each of these traits were observed from backcrossing mice that were presumed heterozygous for the mutation which do not display a phenotype, with an affected parent (N2 backcross), inbred with siblings (affected or not) or crossing two affected animals. Assuming a single autosomal locus was affected, we would expect to see at least 50% of the pups to have a phenotype for a recessive allele based on the predicted genotype of their parents. Since only 20% of the born pups had a discernable phenotype, we hypothesize that these traits are correlated to a common defect occurring earlier during development.

Cranial cephaloceles are defined as sac-like protrusions through a defective opening in the skull. Skulls from affected pups had a broader interfrontal suture space, whether they had a cephalocele, midfacial cleft or both (Figure 1E-H). The frontal bones were diminutive or lacking in rare cases when the cephalocele was large. We also noted that the frontal and parietal bones overlapped each other slightly in most cases, reminiscent of mouse models for craniosynostosis (Figure 1F, H). Since we did not consistently see this in all affected pups, it remains unclear whether this was due to a defect or artifact from preparing skulls for staining.

2. Midline cranial defects originated during fetal development

The occurrence of midfacial clefts and cranial cephaloceles in newborns indicated they arose earlier during development. Examination of embryos revealed that each of these defects first appeared at different stages of development. Evidence of a cyst or hematoma erupting from the head was not clearly evident in embryos until E14.5 or later. They appeared as a transparent bubble or swelling of varying size along the anterior midline of the head (Figure 2A). Coronal sections indicated that the translucent cyst was a swelling of the surface ectoderm over an area corresponding to the sagittal sinus between the cerebral hemispheres (Figure 2B, C). It appeared to be filled with amorphous fluid-like substance or cellular debris. The area comprising the anterior head mesenchyme between the olfactory bulbs was notably broader and appeared to compress the nasal capsule in embryos with the cyst positioned near the rostrum as indicated by a compacted nasal septum.

Embryos with midfacial clefts were easily distinguishable by E12.5 when the medial nasal prominences were fused at the midline in normal appearing littermates. Midfacial clefts could be detected as early as E11.0 in severe cases (Figure 2D). We also found embryos with the anterior part of their forebrain exposed or complete exencephaly during these stages (Figure 2E, F), indicating a failure in neural tube closure.

Horizontal histological sections revealed that the neuroectoderm at the level of the eyes and just above the nasal field remained close or juxtaposed to the surface ectoderm in E11.5-12.5 embryos with a midfacial cleft compared to normal appearing littermates or from 3H1 wildtype mice (Figures 2G-L). The neuroepithelium did not appear to have fused completely as indicated by immunostaining for laminin (Figure 2H, I). N-cadherin was localized along the apical side of the neural tube, but was less prevalent in areas between the neural tips that did not appear to adhere (Figure 2J), while other regions of the neural tube were closed (not shown). In severe cases, the anterior boundary of the neuroepithelium was juxtaposed and remained connected with the surface ectoderm via laminin, such that the third ventricle was vulnerable to rupturing (Figures 2K, L). Closure along the rest of the neural tube appeared complete and normal (not shown).

3. Defect in closure of the neural tube attributed to excessive curling and lack of adhesion of the rostral neural folds

We then examined earlier staged embryos and found that the neural folds along the rostrum were uneven or curled inwards while they were closed in littermates and 3H1 wildtype staged E9.0, during or following axial turning with 16-20 somites (Figure 3A-D). Despite the rostral defect, elevation, bending and closure of the neural tube along the midbrain and through the posterior neuropore appear to have proceeded normally as indicated in E9.5-10.5 litters. However, some embryos showed exencephaly, which would likely result in prenatal death or born with anencephaly (Figure 3C, D **and** Table 1). Approximately 25% of embryos from matings between an affected parent and a normal-appearing relative that was presumed heterozygous for the *tuft* traits exhibited a neural tube defect (Table 1). This is half of what would be expected for an autosomal recessive trait from such mating and predicted genotypes, assuming a single locus was affected.

The rostral defect was also visualized by whole mount *in situ* hybridization (WMISH) of riboprobes for anterior-expressed genes. Fgf8 was prominently expressed along the anterior neural ridge (ANR) in 3H1 wildtype E9.0 embryos (16-20 somites) following neural tube closure (Figure 3E), while it marked the tips of neural folds curling inwards in affected *tuft* embryos (Figure 3F). Fgf8 expression was detected at the base where the neural tube failed to close, approximating the ANR, in later staged litters (Figure 3G). Riboprobes for Shh marked the floor plate or ventral midline of the neural tube and ectoderm along the maxilla between the nasal prominences in both wildtype and affected embryos with little distinction (data not shown). Dense staining in the ectoderm along the midline of the maxilla between the nasal prominences indicated that the rostral closure site near Rathke's Pouch was vulnerable to disruption in some affected embryos (Figure 3H). Elevated or ectopic staining along the ridge of ectoderm corresponding to the dorsal part of the neural tube was also seen in embryos with incomplete closure of the neural tube or exencephaly.

Histological sections of affected E9.0 embryos clearly showed that the rostral folds curled inwards into the neural cavity (Figure 3I-K). Opposing neural folds made contact, but did not adhere to enclose the neural tube. In some cases, they did not appear to make contact, yet proceeded to curl inwards. Since we observed insufficient adhesion of the anterior neural tube in E11.5 embryos with a midfacial cleft and that anterior closure is thought to be initiated by neuroepithelia (Geelen and Langman 1977, 1979), we tried to determine whether cellular adhesion was affected by examining immunohistological stains for cellular adhesion molecules. Immunolocalization of antibodies to E-cadherin (Figure 3J) and N-cadherin (Figure 3K, L) did not reveal compelling anomalies in terms of their prevalence from normal appearing embryos. Yet, adhesion appeared to have failed or was insufficient as seen in E11.5 embryos with a cleft. This indicates that other adhesion factors play a significant role in closure along the rostral neural tube.

Discussion

The etiology of FND is thought to be a developmental field defect affecting features along the frontonasal midline during morphogenesis of the facial bones and tissues (DeMeyer 1967; Sedano 1970; Cohen et al., 1995; Wu et al., 2007; Guion-Almeida and Richieri-Costa 2009). Cephaloceles, cranium bifidum, ocular hypertelorism, a bifid nose and midfacial cleft are features of FND that were observed in the *tuft* mouse (Fong et al., 2012). Consistent with the clinical manifestations of FND, each of these traits in *tuft* mice did not necessarily occur together in the same animal, nor did they occur to the same degree. Cephaloceles, in mice that did not exhibit other craniofacial malformations such as ocular hypertelorism or a bifid nose, were relatively small and positioned further from the rostrum or nasal field. In contrast, mice with a cephalocele proximal of the nasal field almost always exhibited a craniofacial malformation. Mice with a craniofacial malformation, however, did not always have a visible cephalocele. Though these traits can occur together, their separate occurrence suggests they may be caused by a defect affecting a regulatory gene or element influencing multiple developmental mechanisms.

The pathogenesis of how cranial cephaloceles are formed is not understood and whether they originate from a defect during neural tube closure remains an argument. The *tuft* mouse

is the only mammalian model known to exhibit an anterior cranial cephalocele that is heritable. We found that the cephalocele arose as a cyst early as stage E14.5 in *tuft* mice, and later became filled with fat tissue comprising a lipomatous mass. This stage coincides with the genesis of cerebral spinal fluid (CSF) and maturation of the meninges (McLone and Bondareff 1975). Histological analysis of *tuft* mice with cysts indicated that CSF pushed against a simple layer of ectoderm prior to complete ossification of the frontal bones and maturation of the interfrontal suture. Although the cause of CSF accumulation is currently unknown, localized suture patency may be caused by pressure pushing against the dura mater and thin layer of mesenchyme separating the neural tube and surface ectoderm. A barrier between the dura and cranial suture resulted in increased patency and delayed fusion of rat calvarial bones (Roth et al., 1996; Levine et al., 1998). Osteogenesis and suture development of the calvaria depends on the underlying meningeal and mesodermal tissue (Opperman 1995; Rice et al., 2003; Zarbalis et al., 2007; Vivatbutsiri et al, 2008). Thus, signal molecules mediating osteogenesis and suture fusion may be locally disrupted in *tuft* mice, resulting in the cranial bone defect.

The cranial bone defect may be correlated with disturbances occurring earlier during craniofacial development in *tuft* embryos. We found that the neural tube in E11.5-12.5 embryos with a midfacial cleft did not completely fuse or separate from the surface ectoderm along the level of the anterior closure site, compared with 3H1 wildtype mice. Upon neural tube closure, the basal lamina along the surface ectoderm and underlying neuroectoderm remains continuous until the junction is remodeled to form separate basement membranes (Hoving et al., 1990). Closure and separation of the prosencephalic vesicle from the frontonasal ectoderm is mostly complete by stage E9.5-10 in the mouse. A switch in expression of E-cadherin to N-cadherin in the Xenopus neuroectoderm has been shown to be essential for the separation and development of the neural tube (Fujimori et al., 1990). However, the expression of N-cadherin appeared to be normal in *tuft* embryos except in areas where there was a lack of adhesion between the neuroepithelia. So, a switch in expression from E- to N-cadherin along the neuroepithelium did not appear to be affected despite not separating from the frontonasal ectoderm in *tuft* embryos compared to wildtype. This location approximates the anterior neuropore just above the nasal field between initial Closure site 2 at the midbrain and rostral Closure site 3 (Greene and Copp 2009). Incomplete closure and separation of the neuroectoderm from the surface ectoderm along this area would conceivably result in the lack of mesenchyme populating the frontonasal region (Jiang et al., 2002; Yoshida et al., 2008). This deficiency may account for defects in ossification and suture fusion of the calvaria, thus resulting in cranial bifidum and allowing a cephalocele to protrude (Suwanwela and Suwanwela 1972; Hoving and Vermeij-Keers 1997; Han et al., 2007). Incomplete or delayed closure of the neural tube may allow pressure from CSF to push against the weakened neuroectoderm and thinner mesodermal layer, resulting in a cyst (Figure 4A). This is supported by our observation that the neuroectoderm was still associated with the surface ectoderm via laminin in severe cases and thus would be vulnerable to rupture.

The cause for the midfacial cleft in *tuft* embryos is not known. Facial patterning can be dictated by relative levels of Hedgehog signaling between the forebrain and surface

ectoderm. Sonic hedgehog (Shh) expressed from the neuroectoderm of the ventral forebrain elicits it's own expression in a defined region of the frontonasal surface ectoderm, known as the frontonasal ectodermal zone (FEZ), through its receptor Patched and Gli protein transducers in primary cilium of the facial mesenchyme (reviewed in Zaghloul and Brugmann 2011). Conditional knockdown of Shh expression in the FEZ resulted in the merging of lateral elements such as the eyes and nasal prominences toward the center leading to ocular hypotelorism or holoprosencephaly in the most extreme cases (reviewed in Marcucio et al., 2011). In contrast, ectopic levels of Shh, through a conditional loss of Kif3a primary cilia protein, resulted in the opposite phenotype, leading to hypertelorism and bifid nose (Brugmann et al., 2010). In *tuft* embryos with a midfacial cleft, a larger area of head mesenchyme was situated on either side of the neuroectoderm that was near or against the surface ectoderm at the midline (Figure 4B). This dual field may result in a broader domain for Shh signaling in the FEZ by means of increased activity by Gli proteins in head mesenchyme, promoting nasal outgrowth and limiting the ability for nasal prominences to merge toward the midline. A larger area of head mesenchyme was also seen between the olfactory bulbs of embryos with a midline cyst. This may also create a broader expression domain of Shh signaling and thus result in a milder facial malformation such as ocular hypertelorism.

Insufficient closure of the neural tube seen in E11.5 animals can be traced earlier to more severe closure defects seen in E9 embryos. Closure along the rostral or anterior part of the neural tube was affected. The neural folds curled inwards and did not adhere. Closure along the prosencephalon, particularly in the region of the anterior neuropore, appears to be initiated by neuroepithelial cells as opposed to flattened surface epithelia that was observed along the rhombencephalon by transmission electron microscopy (Geelen and Langman 1977, 1979). Immunostainings for E-cadherin, N-cadherin and filamentous actin did not detect obvious differences in their spatial distributions from normal embryos undergoing closure. This suggests that other adhesion molecules such as claudins and ephrins (Holmberg et al., 2000) are likely to play a significant role during closure of the rostral neural tube in *tuft* mice. Mutations in the Graineyhead-like 2 (Grhl2) gene resulted in the downregulation of E-cadherin and claudins in mouse embryo heads (Werth et al., 2010; Pyrgaki et al., 2011). We have yet to also examine the expression of proteins such as BMPs (Furuta et al., 1997), Zic5 (Inoue et al., 2004), and Snail2, that are normally expressed in neural plate border cells corresponding to the dorsal tips during closure along the midbrain (reviewed in Stuhlmiller and García-Castro 2012). Alternatively, curling of the neural folds may have resulted in their inability to adhere. Bending to form hinge points along the midbrain and spine have been shown to be regulated by BMP signaling (Ybot-Gonzalez et al., 2007; Eom et al., 2012). Excessive bending may prevent formation of adhesion complexes in a timely manner in *tuft* embryos. Our model shows that defective closure of the rostral end of the neural tube can lead to prenatal death in mice.

We've identified a candidate region on mouse Chromosome 10 that contain several loci associated with cellular adhesion (Fong et al., 2012). Most notably is Alx1, which along with Alx3 and Alx4, were found mutated in humans with FND-like defects (Kayserili et al., 2009; Twigg et al., 2009; Uz et al., 2010). We did not observe the lack of head mesenchyme

in coronal sections of *tuft* embryos upon closure at E9.0 (data not shown, see Figure 3I) that was characteristically missing in embryos deficient of Alx1 (Zhao et al., 1996). Furthermore, the majority of *tuft* embryos at E9 with a NTD appeared restricted to closure of the anterior or rostral part of the neural tube, whereas overall closure of the cranium was affected in about a third of the embryos (Table 1). Thus, *tuft* represents a novel locus associated with neural tube closure differing from the Alx models for FND. Identifying the genes affected in *tuft* mice will lead to understanding a critical aspect of neural tube closure such that we may develop strategies to remedy or prevent the occurrence of cranial cephaloceles.

Acknowledgments

This work was supported by grants from the Hawai'i Community Foundation (13ADVC-60316 to K. Fong) and National Institutes of Health (1R01-DK-064752 to S. Lozanoff). Use of the Histopathology Core at the John A. Burns School of Medicine was supported by grants from the National Institute on Minority Health and Health Disparities (G12 MD007601) and the National Institute of General Medical Sciences (P30 GM103341). We would also like to extend our thanks to Cliff Tabin and Ralph Marcucio for providing cDNA templates to generate Fgf8 and Shh riboprobes. Special thanks go to Caroline Lau, Lauren Kida and Trudy Hong for their technical contributions as well.

References

Brugmann SA, Allen NC, James AW, Mekonnen Z, Maden E, Helms JA. A primary cilia-dependent etiology for midline facial disorders. Hum Mol Genet. 2010; 19(8):1577–1592. [PubMed: 20106874]

Cohen MM, Lemire RJ. Syndromes with cephaloceles. Teratology. 1982; 25:161–172. [PubMed: 7101196]

Cohen MM, Richieri-Costa A, Guion-Almeida ML, Saavedra D. Hypertelorism: interorbital growth, measurements, and pathogenetic considerations. Int J Oral Maxillofac Surg. 1995; 24:387–395. [PubMed: 8636632]

Cohen MM. Malformations of the craniofacial region: Evolutionary, embryonic, genetic, and clinical perspectives. Am J Med Genet (Semin Med Genet). 2002; 115:245–268.

Correia KM, Conlon RA. Whole-mount in situ hybridization to mouse embryos. Methods. 2001; 23:335–338. [PubMed: 11316434]

DeMyer W. The median cleft face syndrome: differential diagnosis of cranium bifidum occultum, hypertelorism, and median cleft nose, lip, and palate. Neurology. 1967; 17:961–971. [PubMed: 6069608]

Dutta HK, Deori P. Anterior encephaloceles in children of Assamese tea workers. J Neurosurg Pediatrics. 2010; 5:80–84.

Eom DS, Amarnath S, Fogel JL, Agarwala S. Bone morphogenetic proteins regulate hinge point formation during neural tube closure by dynamic modulation of apicobasal polarity. Birth Defects Res Part A. 2012; 94:804–816.

Fong KSK, Cooper TB, Drumhiller WC, Somponpun J, Yang S, Ernst T, Chang L, Lozanoff S. Craniofacial features resembling frontonasal dysplasia with a tubulonodular interhemispheric lipoma in the adult 3H1 *tuft* mouse. Birth Defects Res (Part A). 2012; 94:102–13.

Fujimori T, Miyatani S, Takeichi M. Ectopic expression of N-cadherin perturbs histogeneis in Xenopus embryos. Development. 1990; 110:97–104. [PubMed: 2081473]

Furuta Y, Piston DW, Hogan BLM. Bone morphogenetic proteins (BMPs) as regulators of dorsal forebrain development. Development. 1997; 124:2203–2212. [PubMed: 9187146]

Geelen JAG, Langman J. Closure of the neural tube in the cephalic region of the mouse embryo. Anat Rec. 1977; 189:625–640. [PubMed: 596653]

Geelen JAG, Langman J. Ultrastructural observations on closure of the neural tube in the mouse. Anat Embryol. 1979; 156:73–88. [PubMed: 453553]

Greene NDE, Copp AJ. Development of the vertebrate central nervous system: formation of the neural tube. Prenat Diagn. 2009; 29:303–311. [PubMed: 19206138]

Guion-Almeida ML, Richieri-Costa A, Saavedra D, Cohen MM. Frontonasal dysplasia: analysis of 21 cases and literature review. Int J Oral Maxillofac Surg. 1996; 25:91–97. [PubMed: 8727576]

Guion-Almeida ML, Richieri-Costa A. Frontonasal dysplasia, severe neuropsychological delay, and midline central nervous system anomalies: report of 10 Brazilian male patients. Am J Med Genet Part A. 2009; 149A:1006–1011. [PubMed: 19365836]

Han J, Ishii M, Bringas P Jr, Maas RL, Maxson RE, Chai Y. Concerted action of Msx1 and Msx2 in regulating cranial neural crest cell differentiation during frontal bone development. Mech Dev. 2007; 124:729–745. [PubMed: 17693062]

Harris MJ, Juriloff DM. An update to the list of mouse mutants with neural tube closure defects and advances toward a complete genetic perspective of neural tube closure. Birth Defects Res (Part A). 2010; 88:653–669.

Holmberg J, Clarke DL, Frisén J. Regulation of repulsion versus adhesion by different splice forms of an Eph receptor. Nature. 2000; 408:203–206. [PubMed: 11089974]

Hoving EW, Vermeij-Keers C, Mommaas-Kienhuis AM, Hartwig NG. Separation of neural and surface ectoderm after closure of the rostral neuropore. Anat Embryol. 1990; 182:455–463. [PubMed: 2291490]

Hoving EW, Vermeij-Keers C. Frontoethmoidal encephaloceles, a study of their pathologies. Pediatr Neurosurg. 1997; 27:246–256. [PubMed: 9620002]

Inoue T, Hatayama M, Tohmonda T, Itohara S, Aruga J, Mikoshiba K. Mouse Zic5 deficiency results in neural tube defects and hypoplasia of cephalic neural crest derivatives. Dev Biol. 2004; 270:146–162. [PubMed: 15136147]

Jiang X, Iseki S, Maxson RE, Sucov HM, Morriss-Kay GM. Tissue origins and interactions in the mammalian skull vault. Dev Biol. 2002; 241:106–116. [PubMed: 11784098]

Kayserili H, Uz E, Niessen C, Vargel I, Alanay Y, Tuncbilek G, Yigit G, Uyguner O, Candan S, Hamza Okur, Kaygin S, Balci S, Mavili E, Alikasifoglu M, Haase I, Wollnik B, Akarsu NA. ALX4 dysfunction disrupts craniofacial and epidermal development. Hum Mol Genet. 2009; 18(22):4357–4366. [PubMed: 19692347]

Levine JP, Bradley JP, Roth DA, McCarthy JG, Longaker MT. Studies in cranial suture biology: regional dura mater determines overlying suture biology. Plast Reconstr Surg. 1998; 101:1441–1447. [PubMed: 9583471]

Logan CV, Abdel-Hamed Z, Johnson CA. Molecular genetics and pathogenic mechanisms for the severe ciliopathies: insights into neurodevelopment and pathogenesis of neural tube defects. Mol Neurobiol. 2011; 43:12–26. [PubMed: 21110233]

Lufkin T. In situ hybridization of whole-mount mouse embryos with RNA probes:Hybridization, washes, and histochemistry. Cold Spring Harb Protoc. 2007; 2007:4823.

Mahapatra AK, Agrawal D. Anterior encephaloceles: A series of 103 cases over 32 years. J Clin Neurosci. 2006; 13:536–539. [PubMed: 16679016]

Marcucio RS, Young NM, Hu D, Hallgrimsson B. Mechanisms that underlie co-variation of the brain and face. Genesis. 2011; 49:177–189. [PubMed: 21381182]

McLone DG, Bondareff W. Developmental morphology of the subarachnoid space and contiguous structures in the mouse. Amer J Anat. 1975; 142:273–293. [PubMed: 1119412]

Opperman LA, Passarelli RW, Morgan EP, Reintjes M, Ogle RC. Cranial sutures require tissue interactions with dura mater to resist osseous obliteration in vitro. J Bone Miner Res. 1995; 10:1978–1987. [PubMed: 8619379]

Pyrgaki C, Liu A, Niswander L. Grainyhead-like 2 regulates neural tube closure and adhesion molecule expression during neural fold fusion. Dev Biol. 2011; 353:38–49. [PubMed: 21377456]

Rice R, Rice DPC, Olsen BR, Thesleff I. Progression of calvarial bone development requires Foxc1 regulation of Msx2 and Alx4. Dev Biol. 2003; 262:75–87. [PubMed: 14512019]

Roth DA, Bradley JP, Levine JP, McMullen HF, McCarthy JG, Longaker MT. Studies in cranial suture biology: Part II. Role of the dura in cranial suture fusion. Plast Reconstr Surg. 1996; 97:693–699. [PubMed: 8628762]

Rowland CA, Correa A, Cragan JD, Alverson CJ. Are encephaloceles neural tube defects? Pediatrics. 2006; 118:916–923. [PubMed: 16950981]

Sedano HO, Cohen MM, Jirasek J, Gorlin RJ. Frontonasal dysplasia. J Pediatr. 1970; 76:906–913. [PubMed: 5444583]

Sertie AL, Sossi V, Camargo AA, Zatz M, Brahe C, Passos-Bueno MR. Collagen XVIII, containing an endogenous inhibitor of angiogenesis and tumor growth, plays a critical role in the maintenance of retinal structure and in neural tube closure (Knobloch syndrome). Hum Mol Genet. 2000; 9(13): 2051–2058. [PubMed: 10942434]

Singh AK, Upadhyaya DN. Sincipital encephaloceles. J Craniofac Surg. 2009; 20:1851–1855. [PubMed: 19816364]

Stuhlmiller TJ, García-Castro MI. Current perspectives of the signaling pathways directing neural crest induction. Cell Mol Life Sci. 2012; 69:3715–3737. [PubMed: 22547091]

Suwanwela C, Suwanwela N. A morphological classification of sinsipital encephalomeningoceles. J Neurosurg. 1972; 36:201–211. [PubMed: 5008734]

Theiler, K. The House Mouse: Atlas of embryonic development. Springer-Verlag; New York: 1989.

Thompson DNP. Postnatal management and outcome for neural tube defects including spina bifida and encephaloceles. Prenat Diag. 2009; 29:412–419.

Twigg SRF, Versnel SL, Nurnberg G, Lees MM, Bhat M, Hammond P, Hennekam RCM, Hoogeboom AJM, Hurst JA, Johnson D, Robinson AA, Scambler PJ, Gerrelli D, Nurnberg P, Mathijssen MJ, Wilkie OM. Frontorhiny, a distinctive presentation of frontonasal dysplasia caused by recessive mutations in the ALX3 homeobox gene. Am J Hum Genet. 2009; 84:698–705. [PubMed: 19409524]

Uz E, Alanay Y, Aktas D, Vargel I, Gucer S, Tuncbilek G, von Eggeling F, Yilmaz E, Deren O, Posorski N, Ozdag H, Liehr T, Balci S, Alikasifoglu M, Wollnik B, Akarsu NA. Disruption of ALX1 causes extreme microphthalmia and severe facial clefting: expanding the spectrum of autosomal-recessive ALX-related frontonasal dysplasia. Am J Hum Genet. 2010; 86:789–796. [PubMed: 20451171]

Vivatbutsiri P, Ichinose S, Hytonen M, Sainio K, Eto K, Iseki S. Impaired meningeal development in association with apical expansion of calvarial bone osteogenesis in the Foxc1 mutant. J Anat. 2008; 212:603–611. [PubMed: 18422524]

Werth M, Walentin K, Aue A, Schonheit J, Wuebken A, Pode-Shakked N, Villanovitch L, Erdmann B, Dekel B, Bader M, Barasch J, Rosenbauer F, Luft FC, Schmidt-Ott KM. The transcription factor grainyhead-like 2 regulates the molecular composition of the epithelial apical junctional complex. Development. 2010; 137:3835–3845. [PubMed: 20978075]

Wu E, Vargevik K, Slavotinek AM. Subtypes of frontonasal dysplasia are useful in determining clinical prognosis. Am J Med Genet Part A. 2007; 143A:3069–3078. [PubMed: 17955515]

Ybot-Gonzalez P, Gaston-Massuet C, Girdler G, Klingensmith J, Arkell R, Greene NDE, Copp AJ. Neural plate morphogenesis during mouse neurulation is regulated by antagonism of Bmp signaling. Development. 2007; 134:3203–3211. [PubMed: 17693602]

Yoshida T, Vivatbutsiri P, Morriss-Kay G, Saga Y, Iseki S. Cell lineage in mammalian craniofacial mesenchyme. Mech of Development. 2008; 125:797–808.

Zaghloul NA, Brugmann SA. The emerging face of primary cilia. Genesis. 2011; 49:231–246. [PubMed: 21305689]

Zarbalis K, Siegenthaler JA, Choe Y, May SR, Peterson AS, Pleasure SA. Cortical dysplasia and skull defects in mice with a Foxc1 allele reveal the role of meningeal differentiation in regulating cortical development. Proc Natl Acad Sci. 2007; 104:14002–14007. [PubMed: 17715063]

Zhao Q, Behringer RR, de Crombrugghe B. Prenatal folic acid treatment suppresses acrania and meroanencephaly in mice mutant for the Cart1 homeobox gene. Nat Genet. 1998; 13:275–283. [PubMed: 8673125]

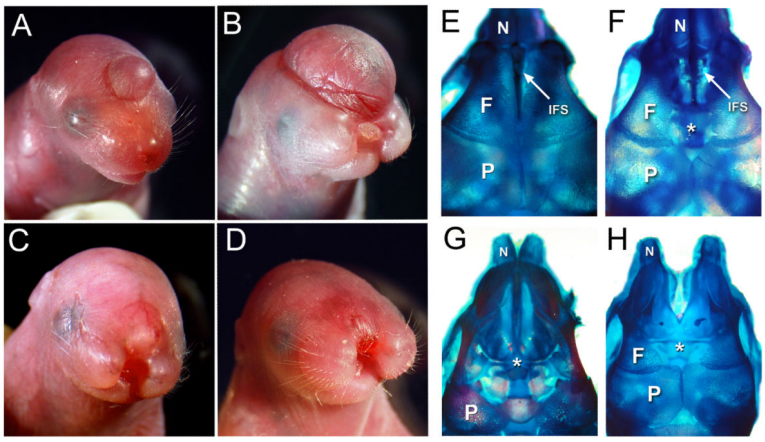

Figure 1.

Cranial traits exhibited by newborn *tuft* mice. **(A)** Anterior cephalocele. **(B)** Large cephalocele and midfacial cleft. **(C, D)** Severe midfacial cleft with an anterior cephaplocele or epidermal lesion (arrow). **(E-H)** Superior views of skulls indicating cranial bone (N, nasal; F, frontal; P, parietal) and suture character from a normal appearing newborn **(E)** compared to it's sibling with a cyst **(F)** that emanated through a broadened interfrontal suture (IFS, arrow) between the frontal bones (asterisk). **(G)** Newborn with a bifid nose and large cephalocele similar in size to pup shown in (B), lacking frontal bones (asterisk). **(H)** Skull from pup with a midfacial cleft and subtle surface lesion or cyst similar to pup shown in (D), also had a broadened IFS (asterisk).

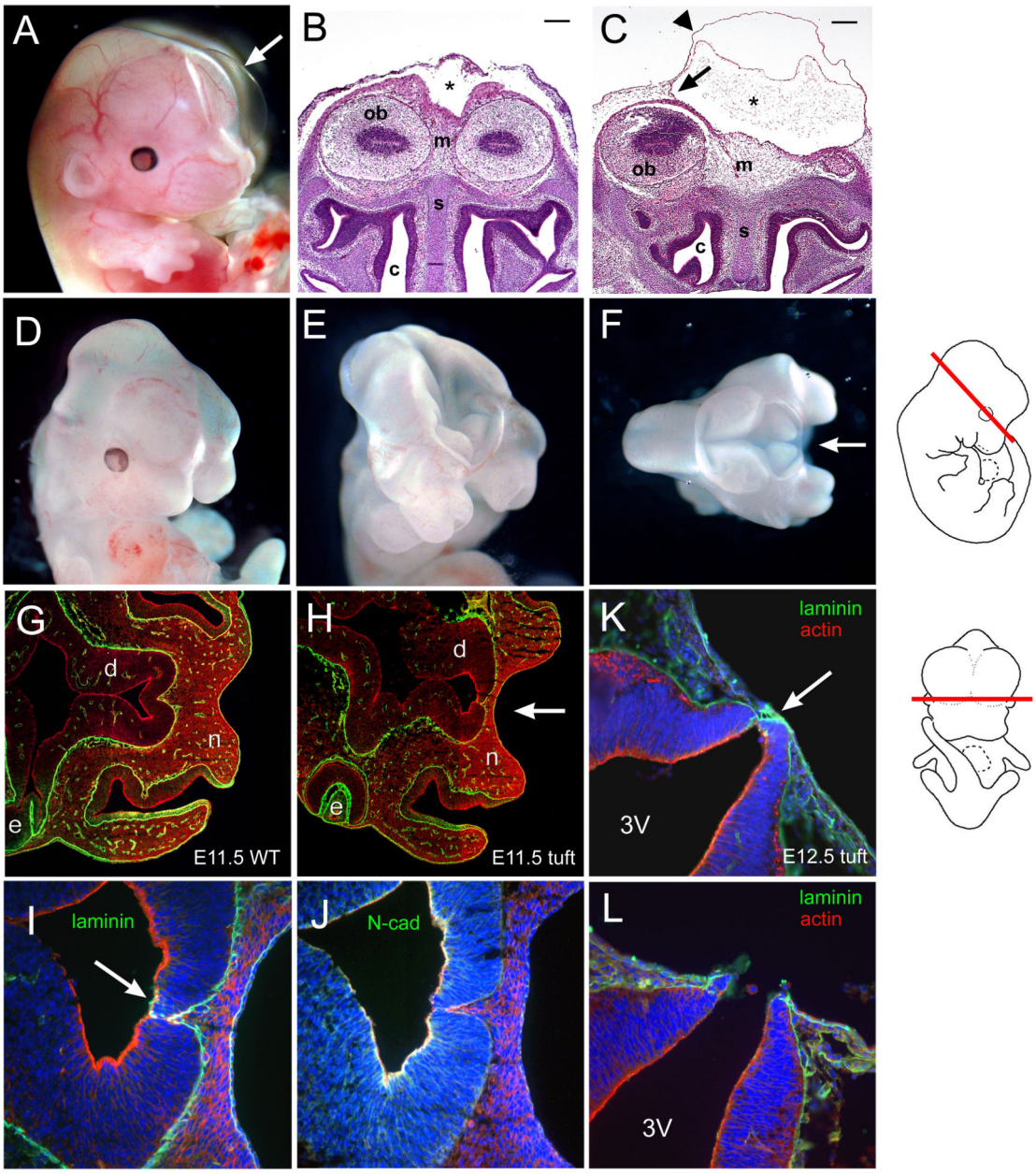

Figure 2.

Cranial malformations in *tuft* embryos. **(A)** E14.5 embryo with a large cyst (arrow). **(B)** Frontal view of an unaffected E14.5 embryo and corresponding section of an **(C)** affected littermate with a cephalocele stained with H & E. The cyst (asterisk) extended the cranial dura meninges (arrow) and outer surface epithelia (arrowhead). Mesenchyme (m), olfactory bulbs (ob), nasal septum (s), and nasal cavity (c) are indicated. Scale bars = 200 microns. **(D)** E11.5 embryo with a midfacial cleft, **(E)** exencephaly and cleft, **(F)** superior view of embryo exposing anterior forebrain and midfacial cleft (arrow). **(G)** Corresponding horizontal sections of 3H1 wildtype E11.5 and **(H)** affected *tuft* embryos with a midfacial cleft (arrow) immunostained for laminin (green) and actin (red) at the level of the

diencephalon (d), eye (e) and nasal prominences (n). Section along the embryo is shown schematically on the right. **(I)** Magnified view of serial sections of (H) immunostained for laminin (green), actin (red) and nuclei (blue) showing insufficient closure (arrow). **(J)** Serial section of (H, I) immunostained for N-cadherin (green), actin (red) and nuclei (blue). **(K, L)** Serial horizontal sections of corresponding levels as (H) in an E12.5 embryo with a midfacial cleft similar to (D) showing the neuroectoderm juxtaposed with the frontonasal ectoderm (arrow) via laminin (green) and exposed third ventricle (3V)**.**

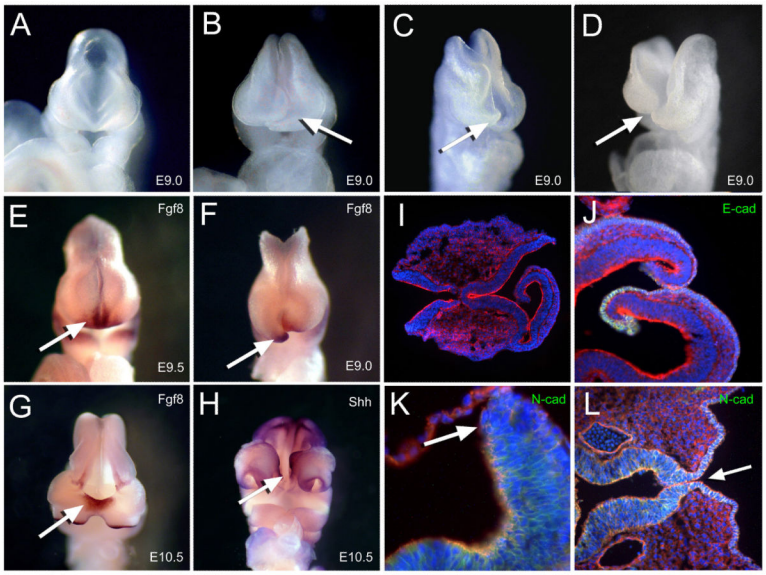

Figure 3.

Neural tube closure was affected along the anterior midline **(A)** Normal appearing E9.0 embryo and **(B-D)** spectrum of affected embryos with crooked or open neural folds along the rostral area (arrow). **(E-G)** Whole mount *in situ* hybridization of riboprobes for Fgf8 as indicated by the dense purple-brown stain marking the ANR (arrows) in **(E)** normal E9.0, **(F)** affected littermate and **(G)** E10.5 embryo with anterior bifidum. **(H)** Ventral view of embryo similar in (G) with dense purple stain marking hybridization of riboprobes for Shh along the ectoderm of the upper lip and floor plate indicating compromised rostral closure site (arrow). **(I)** Horizontal sections of E9 affected embryos immunostained for actin (red) and nuclei (blue) and **(J)** E-cadherin (green) or **(K)** N-cadherin (green). Arrow indicates neural tip lacking stain for N-cadherin in affected embryo. **(L)** Horizontal section of an E10.5 embryo similar to (H) near the neural floor plate immunostained for N-cadherin (green) indicating incomplete closure of the neural epithelium (arrow).

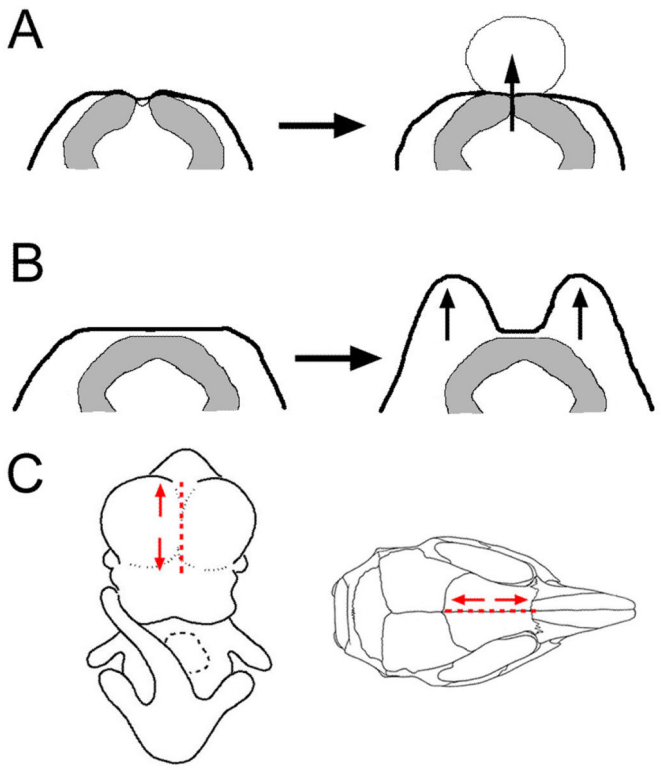

Figure 4.

Craniofacial malformation and cephalocele formation correlated with insufficient neural tube closure. **(A)** In cases when the neural tube failed to adhere completely or did not separate from the surface ectoderm, pressure from CSF could push against the overlying dura and ectoderm, creating a cyst. This locally disrupted ossification, permitting underlying tissue to protrude through a patent interfrontal suture. **(B)** Proximal association of an enclosed neural tube with the surface ectoderm did not permit migration of neural crest cells toward the midline, resulting in larger cell mass lateral of the diencephalon as indicated by horizontal sections in Figure 2. Thus, lateral nasal outgrowth separated by a cleft. **(C)** Dotted line marks the frontonasal midline in embryos and it's corresponding area between the frontal bones where cephaloceles and closure defects were noted. Mice with a cephalocele emanating near the rostrum exhibited a craniofacial malformation, such as a cleft (arrows). Whereas, those that arose further from the nasal field and closer to the parietal bones did not.

Table 1

Occurrence of *tuft* traits in affected newborns (NB) with a midfacial cleft (Clft) with or without cephalocele or anencephaly (*). The occurrence of each trait is indicated as a percentage of the total number of affected NB pups (86). Incomplete closure of the anterior neural tube and exencephaly were scored in litters staged between E9-10.5 as a neural tube defect (NTD). The occurrence of each is likewise indicated as a percentage of affected embryos scored (77).

Phenotype	No. Affected	Total	Litters	%
Affected NB	86	426	64	20.2
Clft w/wo Cephalocele (NB)	32			37.2
Cephalocele (NB)	43			50.0
Anencephaly (NB)	11 (7*)			12.8
Embryos <E10.5 w/ NTD	77	300	43	25.7
Curled rostral neural folds	55			71.4
Exencephaly	22			28.6